Clays and Clay Minerals, Vol. 64, No. 2, 75–85, 2016.

SYNTHESIS OF ZEOLITES FROM A LOW-QUALITY COLOMBIAN KAOLIN

Mónica A. Villaquirán-Caicedo[1,*], Ruby M. de Gutiérrez[1,*], Marisol Gordillo[2], and Nidia C. Gallego[3]

[1] School of Materials Engineering, Composites Materials Group, Universidad del Valle, A.A 25360, Cali, Colombia
[2] Faculty of Sciences, Universidad Autónoma de Occidente, A.A 2790, Cali, Colombia
[3] Oak Ridge National Laboratory, P.O. Box 2008, Oak Ridge, TN, 37831-6087, USA

Abstract—At present, no production of zeolites is ongoing in Colombia; thus, because of the high demand in the industrial sector, ~2500 tons is imported annually from other countries such as Cuba, Ecuador, Mexico, and the United States. In order minimize the need for these costly imports, the present study sought to evaluate the viability of producing low-silica zeolites through the hydrothermal synthesis of a Colombian kaolin, which contains quartz (40%) and iron-oxide impurities. The kaolin was subjected to a milling process to reduce the particle size to the order of 11 μm, and was heat treated to transform it to metakaolin. Optimization of the synthesis variables (Na_2O/SiO_2 and H_2O/Al_2O_3 ratios, time, and temperature) was accomplished by applying an experimental design based on the 'Response Surface Methodology' technique. The degree of crystallinity and the cation exchange capacity (CEC) were used as response variables. The CEC was determined from the NTC 5167 standard. In addition, the mineralogical composition and the zeolite microstructure were evaluated using techniques such as scanning electron microscopy, X-ray diffraction, and solid state nuclear magnetic resonance spectroscopy. The results indicated that synthetic type A zeolites with a CEC value of 442 cmol(+)/kg can be obtained from the Colombian kaolin, with the following optimal processing conditions: Na_2O/SiO_2 molar ratio of 2.7, H_2O/Al_2O_3 molar ratio of 150, temperature = 66ºC, and processing time = 8 h. Note that this value (442 cmol(+)/kg) is greater than that reported for an imported commercial zeolite (408 cmol(+)/kg) of the same type, which is currently being used in industry in Colombia. The nationwide availability of the raw material and the quality of the final product present opportunities to make this material available to the Colombian market.

Key Words—Calcined Kaolin, Cation Exchange Capacity, Hydrothermal Synthesis, Response Surface Methodology, Zeolite A.

INTRODUCTION

Kaolin variously consists of kaolinite-, halloysite-, nacrite-, and dickite-type minerals, accompanied by other components designated as impurities such as quartz, feldspars, micas, and ferric oxides among others. Kaolinite ($Al_2Si_2O_5(OH)_4$), in particular, belongs to the family of phyllosilicates and is formed by sheets of silica tetrahedra and alumina octahedra linked through apical oxygens of the tetrahedral sheet. Kaolin has been used in the production of synthetic zeolites, though these are considered to be of slightly lesser quality than those fabricated with Na aluminosilicate gels, because of the impurities in kaolin (Pavlov *et al.*, 2009) and because they can affect zeolite properties such as the ion-exchange capacity or its degree of whiteness. Kaolin as a raw material reduces substantially the costs of production of synthetic zeolite compared to using chemical reagents as sources of pure silicates and aluminates. Advance treatments of kaolin are necessary, however, to reduce the concentrations of the impurities; *e.g.* an acid treatment at 40ºC is effective at eliminating iron from kaolin, thereby facilitating the synthesis of NaA zeolite which is suitable for use in detergents (Restrepo and Ocampo, 1996). Another difficulty is the poor reactivity of kaolin in synthesis processes (Zhao *et al.*, 2004), which calls for thermal and mechanical activation methods. Heat treatment of kaolin at temperatures between 600 and 1200ºC causes structural transformations attributed to dehydroxylation of the kaolinite structure, obtaining, at ~700ºC, a metastable phase denoted metakaolin ($Al_2Si_2O_7$); at higher temperatures, γ-Al_2O_3 and mullite ($3Al_2O_3.2SiO_2$) are obtained (Restrepo and Ocampo, 1996; Mejía de Gutiérrez and Torres, 2003; Torres *et al.*, 2011). The effects of mechanical or thermal activation of kaolins with different quartz and kaolinite contents were compared by San Cristóbal *et al.* (2010) who found that, during the zeolitization process, the heat-treated samples reacted more quickly and that, although 100% zeolite A was not obtained, the morphology of the cubic crystals was superior.

Different synthesis methods have been employed to obtain zeolites from clays (Novembre *et al.*, 2005; Tavasoli *et al*., 2014), though production from metakaolin (MK) continues to be the method researched most

* E-mail addresses of corresponding authors:
monica.villaquiran@correounivalle.edu.co,
ruby.mejia@correounivalle.edu.co
DOI: 10.1346/CCMN.2016.0640201

widely. Metakaolin, because of its aluminosilicate content and amorphous quality, is highly reactive under alkaline conditions, making it suitable as a raw material in the production of a diverse range of zeolite types (Akolekar *et al.*, 1997; Chandrasekhar *et al.*, 1997; Bobos *et al.*, 2001; Covarrubias *et al.*, 2006; Ríos *et al.*, 2006, 2010; Kuznicki *et al*., 2008; Miao *et al.*, 2009; San Cristobal *et al.*, 2010). These zeolites have been used to adsorb gases such as CO_2, water vapor, and benzene vapor (Chandrasekhar and Pramada, 1999; Pavlov *et al*., 2009), in addition to being useful in controlling industrial waste, *e.g.* in eliminating contaminants such as Cr(III) and radioactive Cs ions from waste waters (Zhao *et al.*, 2004; Covarrubias *et al.*, 2006).

Synthesis of zeolites from MK basically involves two steps: the dissolution of MK, leading to the formation of an aluminosilicate gel, and then nucleation and crystal growth. Among the methods for synthesizing zeolites, the most conventional method, hydrothermal synthesis in an alkaline medium, may be the most important and can be carried out in two or three stages (gelation, aging, and crystallization), but may be carried out by a direct process pathway. Hydrothermal synthesis requires control of the Na_2O/SiO_2 and H_2O/Al_2O_3 ratios in the mixture, temperature, and synthesis time, given that these variables influence the type and quality of the zeolite formed. The quality and type of raw material used are also important. For synthesis of zeolite A, a Si/Al ratio of ~1 and temperatures of <85ºC are recommended; to obtain zeolite X with Si/Al ratios of up to 2.5, the synthesis temperatures used must be greater and other additives are used as sources of silicate, because kaolin alone lacks the Si/Al ratio necessary for the formation of this type of zeolite (Covian-Sanchez, 1991). Products composed of 95% zeolite X and 5% zeolite A have been synthesized in ~20 h periods (Akolekar *et al.*, 1997); zeolite NaX after 24 h of reaction and 87ºC for an SiO_2/Al_2O_3 molar ratio of 3; and thermodynamically metastable mixtures of NaA, NaP, and hydroxysodalite (HS) phases at a SiO_2/Al_2O_3 ratio of 7 (Chandrasekhar and Pramada, 1999). Similarly, zeolite Y has been produced by adding Na silicate as an additional silica source, using synthesis times of >4 h (Chandrasekhar and Pramada, 2004); an aging time of 48 h without an overall gel aging step, and crystallization at 90ºC for 36 h (Tavasoli *et al*., 2014). Low-silica zeolites, such as zeolite A and X, have been obtained (Covarrubias *et al.*, 2006) also by the conventional method in a single stage through addition of Na metasilicate, finding that after 5 h of hydrothermal reaction a mixture of the zeolite phases faujasite and zeolite A occurs and these crystallize simultaneously. After long reaction periods, however, HS is crystallized (<240 h) because it is a more persistent thermodynamic phase; similar results were obtained by other researchers (Akolekar *et al.*, 1997). In addition, reports exist of the synthesis of mordenite-type zeolite with high Si/Al ratios (~20) and ZSM-5 by the seeding technique (Mignoni *et al*., 2008) in which additional Si and Al sources are added to the MK. Two-stage synthesis, the first stage of which consists of aging for 12 h and the second of which consists of crystallization between 70 and 100ºC, has also been researched (Miao *et al.*, 2009). Zeolites A and X were synthesized by Pavlov (2009) by letting the gels age at a temperature between 25 and 30ºC; those authors reported that increasing the aging time from 1 to 24 h had no notable effect on the composition of the phase, crystallinity, nor on adsorption characteristics of the zeolite. In general terms, after 8 h at the crystallization temperature used (95ºC), the zeolite crystallinity remained practically constant. Other methods for zeolite synthesis included ultrasound (Park *et al.*, 2001), which reduces synthesis times and reaction temperature, obtaining products such as zeolite A with a greater degree of crystallinity than that obtained through the conventional method; hydrothermal synthesis with prior fusion in which the kaolin is calcined in NaOH or KOH alkaline solutions at temperatures of ~600ºC followed by conventional synthesis (Ríos *et al.*, 2006, 2010); and microwave synthesis, which uses microwave energy for the initial heating stage during synthesis and – unlike the conventional method – the temperature in the mixture is constant (85ºC) (Chandreskhar and Pramada, 2008).

The objective of the present study was to assess the viability of low-silica zeolite production by hydrothermal synthesis, using heat-treated Colombian kaolin, which has quartz (40%) and iron-oxide impurities. Optimization of the process was achieved through the application of an experimental design based on the Response Surface Methodology (RSM) technique. This statistical method combines experimental design and optimization techniques and establishes the relation between one or more response variables and a group of quantitative factors; furthermore, RSM is a sequential method of experimentation, which presents the alternative of performing a single experiment if the experiment can be extended to take a longer time. For treatments to produce their effects, the natural strategy is to try to discover the optimal combination at the end of the single experiment and, consequently, improve the performance of the process by adjusting variables (Mendez, 1980). In the present study, the Na_2O/SiO_2 and H_2O/Al_2O_3 ratios were optimized, along with time and temperature. For said purpose, a single experiment was developed using RSM in a *Central Composite Design* (Mendez, 1980; Myers *et al*., 2009) in which, in addition, the 2^4 factorial central points and axial points are included. The central points are replicated six times. Based on the results obtained, a prediction model is presented for the value of the CEC as a function of the process variables. The degree of crystallinity (DC) of the zeolite produced is determined and the optimal variables of the synthesis process are defined.

https://doi.org/10.1346/CCMN.2016.0640201 Published online by Cambridge University Press

MATERIALS AND SYNTHESIS OF ZEOLITES

Materials

The kaolin selected for the present study came from the region of Valle del Cauca, Colombia. The chemical composition of kaolin was determined by X-ray fluorescence (XRF) (Table 1). The measured molar ratio of the major oxides (SiO_2/Al_2O_3) present in the kaolin is 2.3, which makes it ideal for obtaining low-silica zeolites (Chandrasekhar and Pramada, 2001; Miao *et al.*, 2009). Based on X-ray diffraction (XRD) analysis, the kaolin contains ~59.5% kaolinite and 40% quartz. The iron oxides, probably present as hematite, were not identified by XRD.

Characterization methods for reactants and products

Prior to the zeolite synthesis, the kaolin was treated mechanically and thermally to obtain MK without chemical intervention. The mechanical treatment consisted of a milling process for a 25 min period using a ball mill (U.S. Stoneware, Model LC-91, Ohio, USA), which yielded an average particle size of 11.7 μm, with 70% of material being <11 μm in size. The particle size was determined by laser granulometry using a Mastersizer 2000 instrument (Malvern Instruments, UK). For thermal treatment, the material was kept at 700ºC for 1 h to release the structural water, thereby obtaining the MK.

The chemical composition of kaolin was measured using a MagixPro PW-2440 X-ray fluorescence spectrometer (PANalytical, USA), equipped with a Rhodium tube with a maximum output of 4.0 kW and 0.02% sensitivity. *SuperQ* software version 5.0L and the *OMNIAN* database of standards were used for the detection and semi-quantitative analysis of elements from sodium (Na) to uranium (U). The powder sample was dried beforehand at 105ºC and then mixed with Merck wax for analysis of the X-ray fluorescence in a 10:1 sample ratio (10 g of sample and 1 g wax); once the sample had homogenized, a hydraulic press at 196 kN was used to generate a pellet 40 mm thick.

Table 1. Chemical composition of kaolin from Valle del Cauca, Colombia.

Component	Wt.%
SiO_2	46.61
Al_2O_3	33.69
TiO_2	1.94
Fe_2O_3	1.18
CaO	0.39
MgO	0.21
K_2O	0.04
SO_3	0.80
LOI	13.54
SiO_2/Al_2O_3 ratio	2.32

LOI denotes loss on ignition.

Thermogravimetric analysis (TGA/DTG) of the samples was performed in a TA Instruments STD Q-600 Simultaneous TGA/DSC instrument (TA Instruments, Newcastle, UK) using alumina crucibles. The test was performed at between 25 and 1250ºC at a heating rate of 10ºC/min with a nitrogen purge rate of 100 mL/min. The software *Universal Analysis 2000* was used to analyze the data (TA Instruments, 2001). The determination of the CEC of the products synthesized was performed using ammonium acetate according to the procedure described in the standard NTC 5167.

The morphological and microstructural analyses were performed by scanning electron microscopy (SEM) using a JEOL JSM-6490LV instrument (JEOL, Japan) , which has an INCAPentaFETX3 detector (Oxford Instruments, model 7573, Oxford, UK). The samples were observed in high-vacuum mode (3×10^{-6} Torr). Images were obtained from powdered samples which were mounted on the sample stubs and sputter-coated with gold.

All solids were identified by X-ray diffraction (XRD) performed on a wide-angle goniometer RINT2000, using the Kα1 signal of Cu at 45 kV and 40 mA, with step size of 0.02º2θ over the range 5−70º2θ at a scan speed of 5º/min. After identifying the type of zeolite, a commercial zeolite 4A Standard QB/T 1768-2003 was used as a reference to determine the DC (degree of crystallinity) based on the XRD pattern, according to ASTM D5357 Standard. This standard is a method for determining the relative crystallinity of zeolite NaA using selected peaks from the XRD pattern of the zeolite.

Solid-state nuclear magnetic resonance (NMR) spectra for ^{29}Si and ^{27}Al were recorded using a Bruker 400 UltraShield™ AVANCE II 400 spectrometer (Bruker Corporation, UK) at a frequency of 59.63 and 78.21 MHz, respectively, and a turning speed of 5 kHz. The spectrum was obtained after irradiation of the sample at a pulse of 5 μs and accumulation time of 5 s.

The TGA curves (Figure 1) of the kaolin indicate an abrupt weight loss, between 400 and 550ºC, corresponding to 13.5%, which is attributed to the loss of hydroxyl groups (OH^-) from the structure. The TGA curve for MK shows variations compared to the same curve for kaolin; in the case of MK, the weight loss was less abrupt (2.4%) and almost constant after 400ºC. The DTA curves for kaolin show the endothermic peak related to dehydroxylation at between 400 and 600ºC (also shown in the TGA), and a small exothermic peak at 1000ºC for the product before the crystallization and formation of a mullite phase. The DTA curve for the MK shows no endothermic peak as pronounced as in the case of kaolin. Slight energy changes occurred throughout the heating, consistent with the nearly constant weight loss. A small exothermic peak at 1000ºC was still observed, reflecting the microstructure modification of the mullite.

The XRD patterns obtained (Figure 2) show the transformation from kaolin to MK; the peaks characteristic of kaolinite (12.14, 19.78, 24.6, and

https://doi.org/10.1346/CCMN.2016.0640201 Published online by Cambridge University Press

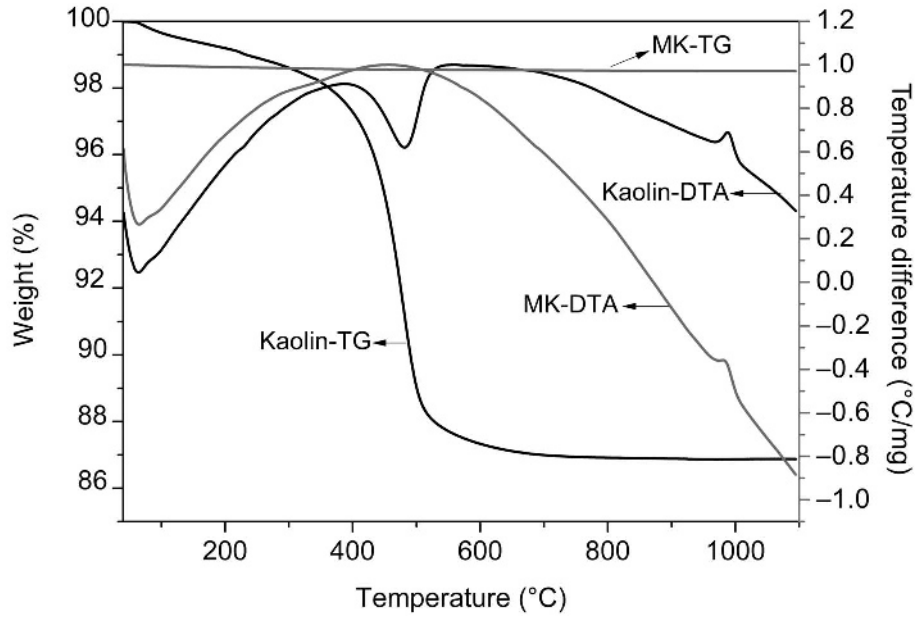

Figure 1. Thermal analysis of the kaolin before and after heat treatment

34.8º2θ) disappeared (Restrepo and Ocampo, 1996; Mejia de Gutierrez and Torres, 2003; Ríos *et al.*, 2006; Torres *et al.*, 2011). The XRD pattern also showed that the MK was not completely amorphous and the characteristic peaks for quartz located at 20.8, 26.6, and 42.3º2θ remained. Scanning electron microscopy images for the kaolin and MK particles (Figure 2) revealed laminar, elongated kaolinite particles, including smaller particles. Only small, agglomerated particles were noted for MK.

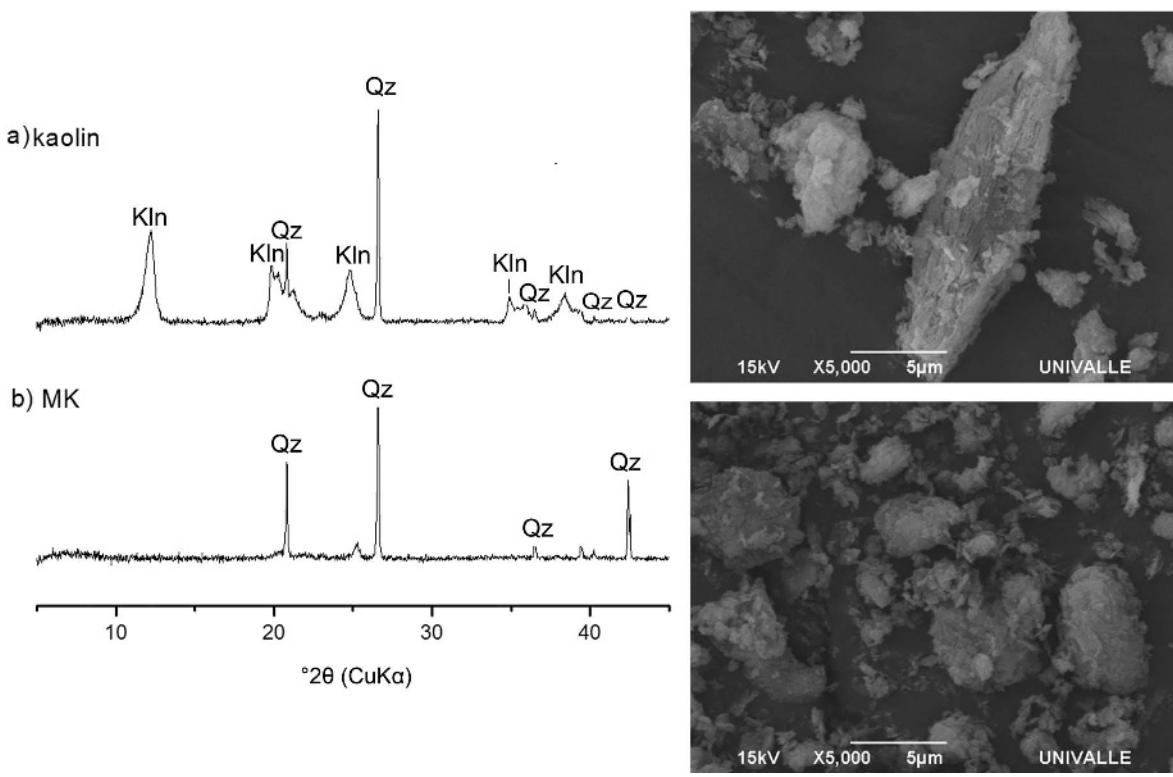

Figure 2. XRD patterns and SEM images of: (a) kaolin and (b) MK (Kln: kaolinite, Qz: quartz).

https://doi.org/10.1346/CCMN.2016.0640201 Published online by Cambridge University Press

Experimental design for the synthesis of zeolites

The zeolites were prepared from MK using the hydrothermal synthesis method with a NaOH alkaline solution. The variables for each trial were determined by experimental design using the RSM technique (Mendez, 1980). With the aid of *Minitab 15* statistics software, a '*Complete Design Central*' was used, in addition to the factorial 2^4, which takes into account a central point that is replicated six times and combinations of central points with factorial points, yielding a total of 31 experiments. The code assigned to each of these was *N*x*W*y*T*z*t*m, where *N* is the Na_2O/SiO_2 molar ratio, *W* is the H_2O/Al_2O_3 molar ratio, *T* is the temperature, and *t* is time. The subscripts x, y, z, and m can each take values of 1, 2, or 3, representing the lower, upper, and central level for each factor; and values of 4 and 0 when they correspond to a mixture of the design (axial points) (Table 2). The ratios used in the present study were *N*: 1.2, 1.7, 2.2; *W*: 75, 100, 125; *T*: 65, 75, 85ºC, *t*: 2, 4, 6 h; in addition, axial points were chosen: *N*: 0.7 and 2.7, *W*: 50 to 150, *T*: 55 and 95ºC, *t*: 1 and 6 h. The response variables selected were the cation exchange capacity (CEC) and the degree of crystallinity (DC).

After the synthesis process, zeolite samples were vacuum-filtered and then washed with distilled water and dried at 103ºC for 12 h prior to the determination of physicochemical and microstructural characteristics.

RESULTS AND DISCUSSION

Results from preliminary samples

CEC and DC. The CEC of zeolites depends on the number of exchangeable cations which is determined by the Si/Al ratio (Covarrubias *et al*., 2006). Zeolite A has a Si/Al ratio of close to 1.0, and the Na^+ ions balance the Al^{3+} ions present in tetrahedral coordination. These Na^+ ions in the zeolite are mobile and can be exchanged for other cations in aqueous solution under certain conditions. The CEC was determined for the 31 samples generated during the experiments. The results obtained for each sample were compared to the raw materials and a commercial zeolite 4A. The kaolin (Figure 3) exhibited a CEC of 40 cmol(+)/kg and thermal activation of the kaolin to obtain the MK reduced this value to 14 cmol(+)/kg. Further hydrothermal activation of the MK with NaOH resulted in an increase in the CEC. Samples with the typical cubic geometry of zeolite A, as determined by SEM and XRD, exhibited greater CEC values; sample 31-*N*3*W*3*T*3*t*3 had a CEC of 403 cmol(+)/kg, a value close to that of the commercial zeolite 4A (408 cmol(+)/kg).

The DC of the zeolites was determined by XRD using equation 1 (also used previously by other authors: Park *et al*., 2001), where *I* represents the intensity of the sample to be evaluated and I_0 is the intensity of the reference sample; in the present case, the commercial zeolite A was assigned a DC value of 100%. The DC was determined as the sum of intensities of strong peaks in the XRD pattern between angles 6 and 40º2θ. A significant number of samples showed high DC values, *e.g.* samples 25-*N*2*W*2*T*2*t*0 and 31-*N*3*W*3*T*3*t*3 had DC values of 76.3 and 79.5%, respectively.

$$DC = \left(\frac{I}{I_0}\right) \times 100 \quad (1)$$

The CEC values obtained were in the range 79.3−403.3 cmol(+)/kg (Figure 3); further analysis of these results through the *Minitab 15* statistical analysis package allowed the establishment of a relation between the DC and CEC values (Figure 4), expressed by

Table 2. Randomization of experiments.

Nº	Sample	*N*	*W*	*T*	*t*	Nº	Sample	*N*	*W*	*T*	*t*
1	*N*1*W*3*T*1*t*3	1.2	125	65	6	16	*N*1*W*1*T*3*t*3	1.2	75	85	6
2	*N*2*W*2*T*2*t*2	1.7	100	75	4	17	*N*0*W*2*T*2*t*2	0.7	100	75	4
3	*N*2*W*2*T*2*t*0	1.7	100	75	0	18	*N*3*W*1*T*3*t*1	2.2	75	85	2
4	*N*1*W*3*T*3*t*3	1.2	125	85	6	19	*N*2*W*2*T*2*t*2	1.7	100	75	4
5	*N*1*W*3*T*3*t*1	1.2	125	85	2	20	*N*2*W*2*T*2*t*2	1.7	100	75	4
6	*N*2*W*2*T*2*t*2	1.7	100	75	4	21	*N*1*W*2*T*3*t*1	1.2	100	85	2
7	*N*3*W*3*T*3*t*1	2.2	125	85	2	22	*N*2*W*2*T*2*t*2	1.7	100	75	4
8	*N*3*W*1*T*1*t*1	2.2	75	65	2	23	*N*1*W*1*T*1*t*3	1.2	75	65	6
9	*N*2*W*2*T*2*t*2	1.7	100	75	4	24	*N*2*W*2*T*2*t*2	1.7	100	75	4
10	*N*3*W*3*T*1*t*1	2.2	125	65	2	25	*N*2*W*2*T*2*t*4	1.7	100	75	8
11	*N*2*W*4*T*2*t*2	1.7	150	75	4	26	*N*4*W*2*T*2*t*2	2.7	100	75	4
12	*N*2*W*2*T*0*t*2	1.7	100	55	4	27	*N*1*W*3*T*1*t*1	1.2	125	65	2
13	*N*2*W*0*T*2*t*2	1.7	50	75	4	28	*N*1*W*1*T*1*t*1	1.2	75	65	2
14	*N*3*W*3*T*3*t*3	2.2	125	85	6	29	*N*3*W*1*T*1*t*3	2.2	75	65	6
15	*N*2*W*2*T*4*t*2	1.7	100	95	4	30	*N*3*W*1*T*3*t*3	2.2	75	85	6
						31	*N*3*W*3*T*1*t*3	2.2	125	65	6

N: Na_2O/SiO_2 molar ratio, *W*: H_2O/Al_2O_3 molar ratio, *T*: temperature, and *t*: time.

https://doi.org/10.1346/CCMN.2016.0640201 Published online by Cambridge University Press

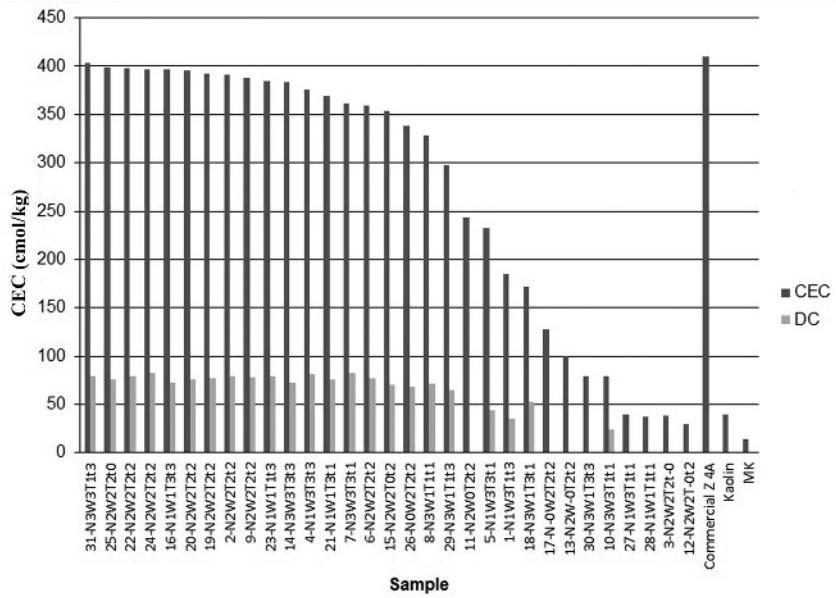

Figure 3. Cation exchange capacity (CEC) (cmol/kg) and degree of crystallinity (DC) (%) for the preliminary products, compared to the raw materials and the commercial zeolite.

equation 2. Based on this equation, which had an R^2 value of 94.8%, prediction of the DC values for samples became possible and values between 8.64 and 50.12% were found (the SEM results did not reveal the typical cubic morphology of the zeolite A), (samples: 3-*N*2*W*2*T*2*t*-0, 11-*N*2*W*0*T*2*t*2, 13-*N*2*W*-0*T*2*t*2, 17-*N*-0*W*2*T*2*t*2, 12-*N*2*W*2*T*-0*t*2, 27-*N*1*W*3*T*1*t*1, 28-*N*1*W*1*T*1*t*1, and 30-*N*3*W*1*T*3*t*3).

$$DC = 2.83 + 0.194\ CEC \quad (2)$$

In this way, the DC of the material can be predicted through the CEC, without using XRD.

Optimization of the RSM and selection of optimum synthesis parameters. Based on statistical analysis of the results of the 31 initial trials (Figure 3), a general model for the CEC was defined and shown in equation 3 (R^2 = 99.3%). In this equation, χ_1, χ_2, χ_3, and χ_4 represent the Na_2O/SiO_2 and H_2O/Al_2O_3 ratios, temperature, and time.

$$CEC_{ijkl} = -4537.09 + 676.55\chi_1 + -13.82\chi_2 + 101.41\chi_3 + 424.21\chi_4 + -93.45\chi_1\chi_1 + \beta - 0.06\chi_2\chi_2 + 0.52\chi_3\chi_3 + -11.26\chi_4\chi_4 + 6.31\chi_1\chi_2 + -11.22\chi_1\chi_3 + 31.34\chi_1\chi_4 + 0.18\chi_2\chi_3 + 0.55\chi_2\chi_4 + -3.88\chi_3\chi_4 + \varepsilon_{ijkl} \quad (3)$$

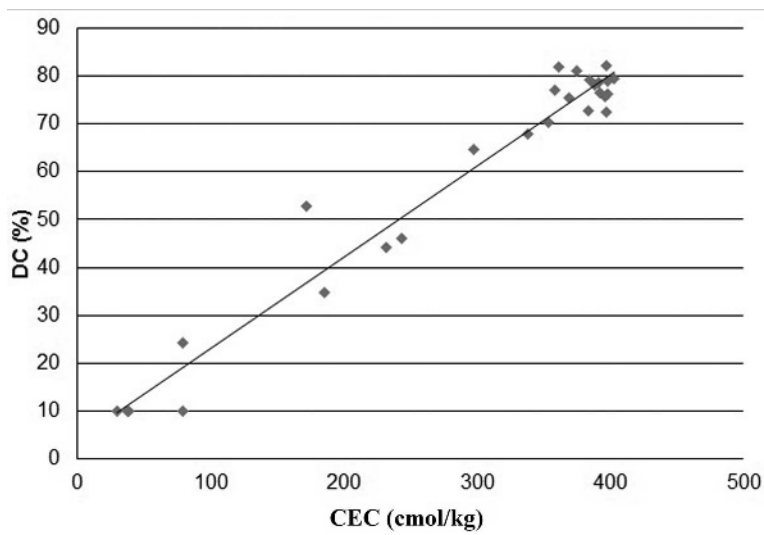

Figure 4. Statistical relationship between CEC and DC.

https://doi.org/10.1346/CCMN.2016.0640201 Published online by Cambridge University Press

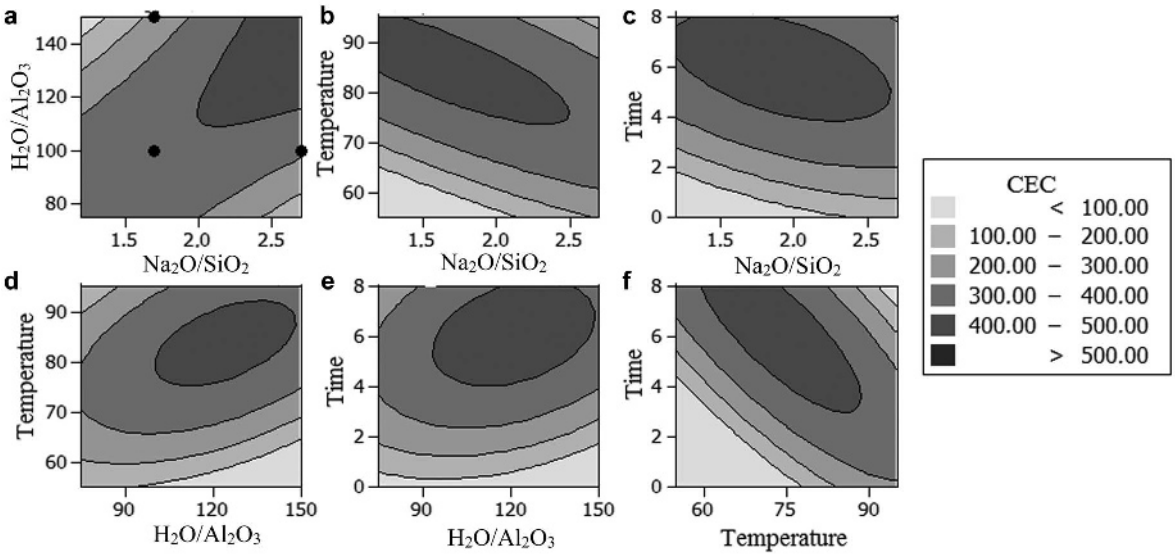

Figure 5. Contour plots of the CEC (cmol(+)/kg) of the preliminary samples.

The experimental behavior shows that if the CEC were to depend on the molar ratios (Na_2O/SiO_2 and H_2O/Al_2O_3) only, these would be directly proportional to the CEC, as shown in the contour plot (Figure 5a). When other variables enter the system, such as temperature and time, the CEC is favored by smaller molar ratios (Na_2O/SiO_2) at higher temperatures and for long periods of time (Figure 5b,c). The second factor (the H_2O/SiO_2 ratio) is also shown to have a significant effect on the CEC, and a maximum CEC was obtained when temperature and time increased, but when the temperature exceeded 90ºC, a decrease in CEC was observed. Time and temperature were shown to act against each other in terms of the CEC (Figure 5d,e,f): temperatures below 75ºC required longer periods to form zeolites with large CEC values; similar results were found by Covian-Sanchez (1991). The optimal values of CEC (between 400 and 500 cmol(+)/kg) were obtained under the following conditions: Na_2O/SiO_2 molar ratio between 2.3 and 2.5; H_2O/SiO_2 molar ratio between 120 and 140; temperature between 85 and 95ºC; and time between 5 and 8 h.

Synthesis parameters and characterization of optimal product

From the application of the RSM, three possible optimizations of variables for zeolite synthesis were generated. These conditions were applied to MK to obtain OPT1, OPT2, and OPT3. The same synthesis parameters were also applied to an imported, commercial source of MK of high purity (Metamax®, BASF Catalyst, New Jersey, USA), and the products obtained were labeled OPT1*, OPT2*, and OPT3* and used for comparison (Table 3). As a benchmark, a commercial zeolite 4A was assessed in the same tests.

The CEC measurement for the samples synthesized under 'optimum' conditions found (Table 4) that the zeolites synthesized from MK, obtained by mechanical and thermal treatment of kaolin, under optimal conditions OPT2 and OPT1, exceeded the CEC value for the commercial zeolite 4A (408 cmol(+)/kg). By increasing the purity of the MK (*i.e.* using the commercial MK, Metamax®), greater CEC values were obtained compared to those predicted by the model by up to 15%, and with a DC of ~100%. The SEM images and XRD patterns (Figure 6) for OPT1 and OPT1* (which had the largest CEC value) were comparable with those of the commercial zeolite 4A. The cubic morphology, characteristic of zeolite A, was observed in these images; the vast majority of the products obtained exhibited cubes with sharp corners, but exceptions were present where the cubes had rounded corners, similar to those obtained by Chunfeng (2009). In general, the cube size was greater for those obtained with the commercial MK under the same synthesis conditions, *e.g.* for OPT1* the cube size was between 1.4 and 1.6 μm,

Table 3. Processing conditions.

Optimal	Molar ratio		*T*	*t*
	Na_2O/SiO_2	H_2O/Al_2O_3	(ºC)	(h)
OPT1/OPT1*	2.7	150	66	8.00
OPT2/OPT2*	2.0	116	72	6.44
OPT3/OPT3*	1.2	75	76	5.46

https://doi.org/10.1346/CCMN.2016.0640201 Published online by Cambridge University Press

Table 4. CEC and degree of crystallinity (DC) of samples produced at optimum conditions.

Sample	CEC (cmol(+)/kg) Predicted	CEC (cmol(+)/kg) Measured	CEC standard deviation (%)	DC (%)
OPT1	503	442	−12.12	88.57
OPT2	444	422	−4.95	84.70
OPT3	441	397	−9.97	79.85
OPT1*	503	506	+0.59	100
OPT2*	444	499	+12.38	99.60
OPT3*	441	507	+14.96	100
Kaolin	–	40	–	–
Metakaolin	–	14	–	–
Commercial Zeolite 4A	–	408	–	100

while for the OPT1 product, the cubes were <1 μm. The presence of some beads, like 'cotton balls,' was also observed for the commercial zeolite 4A, distinguishable from the zeolite PHI or phillipsite (Rios and Williams, 2008; Rios and Denver, 2010). In general, the crystalline product obtained was identified by diffraction angles of zeolite A (Figure 6), corresponding to 10.19, 12.49, 16.14, 21.02, 27.18, and 30.01º2θ with evidence of small amounts of the zeolite, phillipsite (Php), which was identified at 21.51 and 32.44º2θ. In addition, the XRD patterns indicated the presence of quartz (Qz, 20.86 and 26.6º2θ) in the MK. Note that the presence of quartz in the final product does not affect the exchange properties of zeolite because the values obtained were satisfactory and greater than the CEC value of the commercial zeolite 4A. The crystallinity of the OPT1 zeolite was 88.57% and for the OPT1* was considered to be 100%.

Aluminosilicates such as clays and zeolites contain SiO_4 and AlO_6/AlO_4 units, which can be studied by solid-state NMR spectroscopy using the ^{29}Si and ^{27}Al probe. The silicon probe provides information about the type of silicate formed Q^1, Q^2, Q^3, or Q^4, as well as the substitution of this structure in other species; thus, the nomenclature $Q_n(_mAl)$, where n indicates the number of oxygen atoms being shared with another silicate or tetrahedral aluminate and m represents the number of neighboring aluminate groups (Scheneider *et al.*, 2001). The signal for the Si is between −70 and −110 ppm, but its exact position depends on the possible surrounding cations. When using an Al probe, the signal positions depend on the coordination: tetrahedral (+50 to +70 ppm), pentahedral (+30 ppm), or octahedral (−10 to +10 ppm). Nuclear magnetic resonance spectra were obtained (Figure 7) for the starting MK, OPT1, OPT1*,

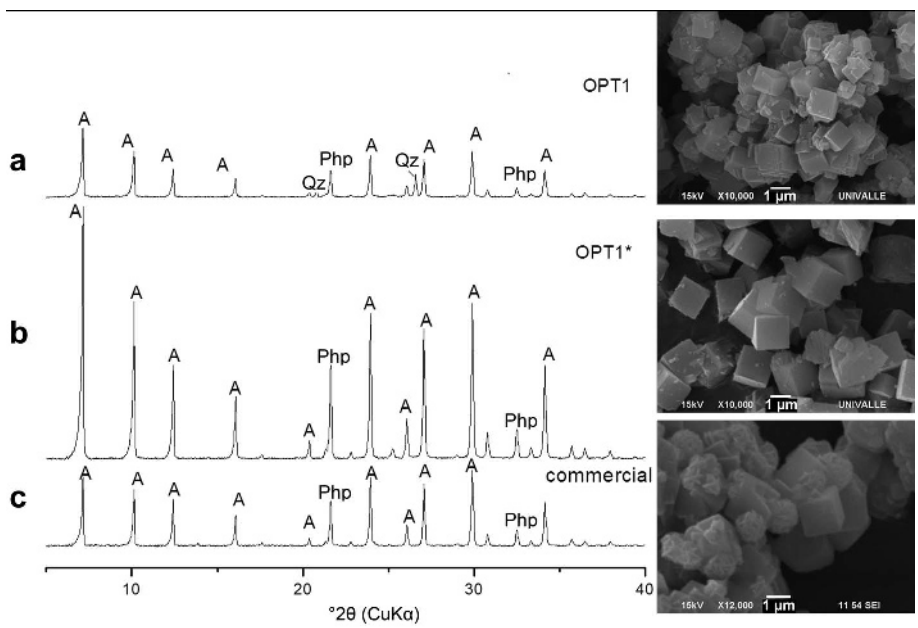

Figure 6. XRD patterns and SEM images of zeolite samples: (a) OPT1; and (b) OPT1* compared to (c) commercial zeolite 4A (Php: phillipsite, Qz: quartz).

https://doi.org/10.1346/CCMN.2016.0640201 Published online by Cambridge University Press

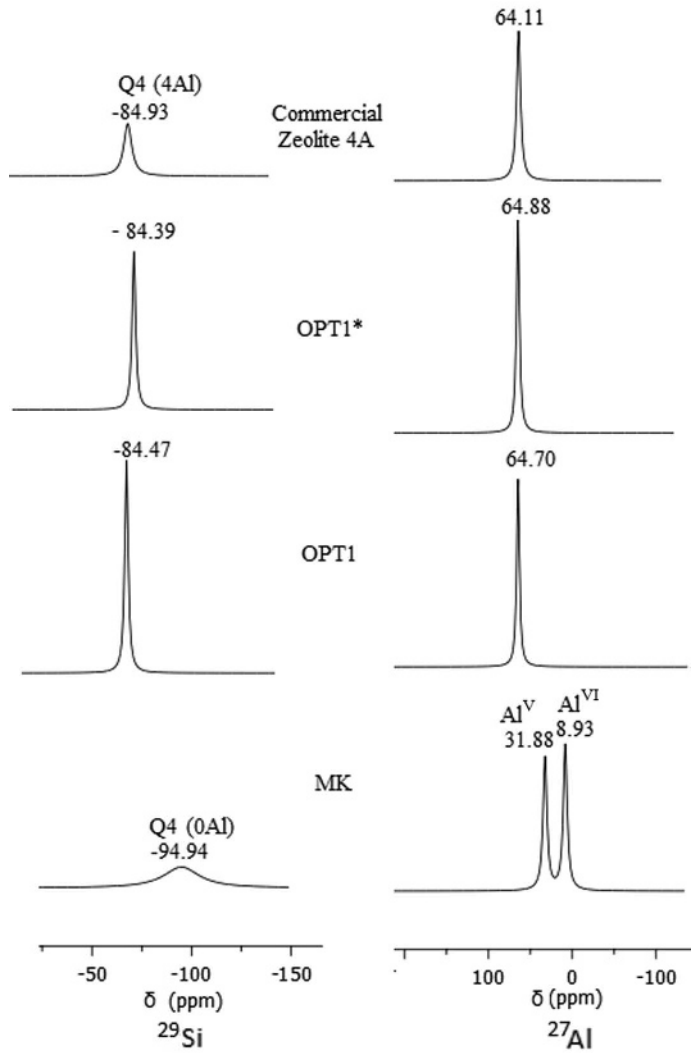

Figure 7. NMR spectra of OPT1 and OPT1* compared to MK and commercial zeolite.

and commercial zeolite 4A. For the MK, signals were observed at +8.9 ppm (Al^{VI}) and +31.38 ppm (Al^{V}) ppm, corresponding to hexa- and penta-coordinated Al in the structure (Chandrasekhar and Pramada, 1999). After the synthesis process, a shift of the signal to the left; now located at ~+64 ppm, was observed in the products, similar to that observed in the commercial zeolite 4A, confirming the presence of mostly Al^{IV} in the final product. As for the spectrum obtained with the probe for ^{29}Si, for the MK a broad signal was noted at ~−94.9 ppm, corresponding to $Q^4(0Al)$ and attributable to silica polymorphs (Thompson and Barron, 1987) and the presence of amorphous silica (Rocha and Klinowski, 1990). With the hydrothermal treatment, the position of the signal was shifted to the left, indicating that the structure of zeolite A was formed by unions of sodalite through four-membered double rings as revealed by characteristic shifts of ~−83, −84, and −85 ppm, which further indicated alteration and maximum degree of isomorphous substitution resulting in the formation of $Q^4(4Al)$ bonds, characteristic of zeolite A (Chandrasekhar and Pramada, 2008; Ríos *et al.*, 2010).

CONCLUSIONS

The feasibility of synthesizing a type A zeolite having a quality comparable to commercially available zeolites, using Colombian raw materials, was demonstrated. The zeolite was produced by hydrothermal treatment of a MK, obtained by mechanical and thermal treatment of Colombian kaolin with a large (40%) quartz content, which does not affect significantly the CEC properties of the zeolites synthesized. The best zeolites obtained were type 4A, which exhibited large CEC values (up to 442 cmol(+)/kg of zeolite), DC values of >85%, and average particle sizes of 1 μm. The optimal process conditions were: H_2O/Al_2O_3 and Na_2O/SiO_2 molar ratios of 2.7 and 150, respectively; a temperature

https://doi.org/10.1346/CCMN.2016.0640201 Published online by Cambridge University Press

of 66ºC; and an 8 h processing time. When these synthesis parameters were applied to a commercial MK of greater purity, the zeolite obtained was also type A, with a slightly greater CEC value (507 cmol/kg). The results presented here (synthesis of zeolite type A, from a Colombian MK, with a resultant quality comparable to commercial zeolite 4A) offer a significant opportunity for industrial production, in Colombia, of a valuable material which is currently imported and in high demand by the national industrial sector.

ACKNOWLEDGMENTS

The present study was supported by Universidad del Valle (Colombia), the Center of Excellence for Novel Materials (CENM), and Departmento Administrativo de Ciencia, Tecnología e Innovación COLCIENCIAS. The participation of author N.C. Gallego was funded by a grant from the Fulbright Colombia Commission.

REFERENCES

Akolekar, D., Chafee, A., and Howe, R.F. (1997) The transformation of kaolin to low-silica X zeolite. *Zeolites*, **19**, 359–265.

ASTM D5357-03 (2013) Standard test method for determination of relative crystallinity of zeolite sodium A by X-ray Diffraction.

Bobos, I., Duplay, J., Rocha J., and Gomez, C. (2001) Kaolinite to halloysite 7 Å transformation in the kaolin deposit of Sao Vicente de Pereira, Portugal. *Clays and Clay Minerals*, **49**, 596–607.

Chandrasekhar, S. and Pramada, P.N. (1999) Investigation on the synthesis of zeolite NaX from Kerala kaolin. *Journal of Porous Materials*, **6**, 283–297.

Chandrasekhar, S. and Pramada, P.N. (2008) Microwave assisted synthesis of zeolite A from metakaolin. *Microporous and Mesoporous Materials*, **108**, 152–161.

Chandrasekhar, S. and Pramada, P.N. (2001) Sintering behavior of calcium exchanged low silica zeolites synthesized from kaolin. *Ceramics International*, **27**, 105–114.

Chandrasekhar, S. and Pramada, P.N. (2004) Kaolin based zeolite Y, a precursor for cordierite ceramics. *Applied Clay Science*, **27**, 187–198.

Chandrasekhar, S., Raghavan, P., Sebastian, G., and Damodaran, A.D. (1997) Brightness improvement studies on "kaolin based" zeolite 4A. *Applied Clay Science*, **12**, 221–231.

Chunfeng, W., Jiansheng, L., Xia, S., Lianjun, W., and Xiuyun, S. (2009) Evaluation of zeolites synthesized from fly ash as potential adsorbents for wastewater containing heavy metals. *Journal of Environmental Sciences*, **21**, 127–36.

Covarrubias, C., García, R, Arriagada, R., Yánez, J., and Garland, M. (2006) Cr(III) exchange on zeolites obtained from kaolin and natural mordenite. *Microporous and Mesoporous Materials*, **88**, 220–231.

Covian-Sanchez, I. (1991) *Síntesis de zeolitas 13X para uso en detergentes*. PhD thesis, Universidad Complutense de Madrid, Madrid, 305 pp.

Kuznicki, S.M., Lin, C.C., Wu, L., Yin, H., Danaie, M., and Mitlin, D. (2008) The synthesis of a platy chabazite analog from delaminated metakaolin with the ability to surface template nanosilver particulates. *Clays and Clay Minerals*, **56**, 655–659.

Mejía de Gutiérrez, R. and Torres, J. (2003) Puzolana obtenida por activación térmica. Pp. 25–29 in: Memorias III Jornadas Iberoamericanas de Materiales de Construcción, Red Iberoamericana de Rocas y Minerales Industriales, XIII-C – CYTED, San Juan, Argentina.

Mendez, I., editor (1980) *Metodología de Superficie de Respuesta*. Instituto de Investigaciones en Matemáticas Aplicadas y en Sistemas, UNAM, Mexico D.F., Mexico, pp. 15–17.

Miao, Q., Zhou, Z., Yang, J., Lu, J., Yan, S., and Wang, J. (2009) Synthesis of NaA zeolite from kaolin source. *Frontiers of Chemical Engineering China*, **3**, 8–11.

Mignoni, M., Petkowicz, D.I., Fernandes, N., and Sibele, B.C. (2008) Synthesis of mordenite using kaolin as Si and Al source. *Applied Clay Science*, **41**, 99–104.

Myers, R.H., Montgomery, D.C., and Anderson-Cook, C.M. (2009) *Response Surface Methodology: Process and Product Optimization using Designed Experiments.* Wiley Series in Probability and Statistics.

Novembre, D., Sabatino, B., and Gimeno, D. (2005) Synthesis of Na-A zeolite from 10 Å halloysite and new crystallization kinetic model for the transformation of Na-A into HS zeolite. *Clays and Clay Minerals*, **53**, 28–36.

NTC 5167 (2004) Productos para la industria agrícola, productos orgánicos usados como abonos y fertilizantes y enmiendas del suelo. Icontec, Colombia.

Park, J., Chan, B., Soo, S., and Chan, H. (2001) Conventional versus ultrasonic synthesis of zeolite 4A from kaolin. *Journal of Materials Science Letters*, **20**, 531–533.

Pavlov, M.L., Travkina, O.S., Basimova, R.A., Pavlova, I.N., and Kutepov, B.I. (2009) Binder-free synthesis of high-performance zeolites A and X from kaolin. *Petroleum*, **49**, 36–41.

Restrepo, G.M. and Ocampo, G.A. (1996) Sustitución de polifosfatos por zeolitas en detergentes. *Revista Facultad Ingeniería Química Universidad de Antioquia*, **13**, 15–20.

Ríos, C.A. and Denver, C.W. (2010) Hydrothermal transformation of kaolinite in the system K_2O-SiO_2-Al_2O_3-H_2O. *DYNA*, **77**, 55–63.

Ríos, C.A. and Williams, C.D. (2008) Synthesis of zeolitic materials from natural clinker: A new alternative for recycling coal combustion by-products. *Fuel*, **87**, 2482–2492.

Ríos, C.A., Williams, C.D., and Castellanos, O.M. (2006) Síntesis y caracterización de zeolitas a partir de la activación alcalina de caolinita y subproductos industriales (cenizas volantes y clincker natural) en soluciones alcalinas. *BISTUA*, **4**, 60–71.

Ríos, C.A., Denver, C.W., and Castellanos, OM. (2010) Synthesis of zeolite LTA from thermally treated kaolinite. *Revista Facultad de Ingenieria Universidad de Antioquia*, **53**, 30–41.

Rocha, J. and Klinowski, J. (1990) ^{29}Si and ^{27}Al magic-angle-spinning NMR studies of the thermal transformation of kaolinite. *Physics and Chemistry of Minerals*, **17**, 179–186.

San Cristóbal, A.G., Castelló, R., Luengo, M.A., and Vizcayno, C. (2010) Zeolites prepared from calcined and mechanically modified kaolins a comparative study. *Applied Clay Science*, **49**, 239–246.

Schneider, J., Cincotto, M.A., and Panepucci, H. (2001) ^{29}Si and ^{27}Al high-resolution NMR characterization of calcium silicate hydrate phases in activated blast-furnace slag pastes. *Cement and Concrete Research*, **31**, 993–1001.

TA Instruments (2001) The software universal analysis. http://www.tainstruments.com/?gclid=CKzMpe6M-MwCFYEehgod3_cEtg

Tavasoli, M., Kazemian, H., Sadjadi, S., and Tamizifar, M. (2014) Synthesis and characterization of zeolite NaY using kaolin with different synthesis methods. *Clay and Clays Minerals*, **62**, 508–518.

Thompson, J.G. and Barron P.F. (1987) Further consideration of the ^{29}Si nuclear magnetic resonance spectrum of

kaolinite. *Clays and Clay Minerals*, **35**, 38–42.
Torres, J., Mejia de Gutiérrez, R., Castelló, R., and Vizcayno, C. (2011) Análisis comparativo de caolines de diferentes fuentes para la producción de metacaolin. *Revista Latinoamericana de Metalurgia y Materiales*, **31**, 35–43.
Zhao, H., Deng, Y., Harsh, J.B., Markus, F., and Boyle, J.S. (2004) Alteration of kaolinite to cancrinite and sodalite by simulated Hanford tank waste: Its impact on cesium retention. *Clays and Clay Minerals*, **52**, 1–13.

(*Received 5 June 2012; revised 4 February 2016; Ms. 677; AE: Steven M. Kuznicki*)